BJR

Received:
23 September 2016

Revised:
11 December 2016

Accepted:
22 December 2016

https://doi.org/10.1259/bjr.20160768

Cite this article as:
Wong KH, Panek R, Bhide SA, Nutting CM, Harrington KJ, Newbold KL. The emerging potential of magnetic resonance imaging in personalizing radiotherapy for head and neck cancer: an oncologist's perspective. *Br J Radiol* 2017; **90**: 20160768.

REVIEW ARTICLE

The emerging potential of magnetic resonance imaging in personalizing radiotherapy for head and neck cancer: an oncologist's perspective

[1,2]KEE H WONG, FRCR, [1,2]RAFAL PANEK, PhD, [1,2]SHREERANG A BHIDE, PhD, [1,2]CHRISTOPHER M NUTTING, PhD, [1,2]KEVIN J HARRINGTON, PhD and [1,2]KATIE L NEWBOLD, MD

[1]Head and neck unit, The Royal Marsden Hospital, London, UK
[2]Radiotherapy and imaging, The Institute of Cancer Research, London, UK

Address correspondence to: Dr Kee H Wong
E-mail: *kee.wong@icr.ac.uk*

ABSTRACT

Head and neck cancer (HNC) is a challenging tumour site for radiotherapy delivery owing to its complex anatomy and proximity to organs at risk (OARs) such as the spinal cord and optic apparatus. Despite significant advances in radiotherapy planning techniques, radiation-induced morbidities remain substantial. Further improvement would require high-quality imaging and tailored radiotherapy based on intratreatment response. For these reasons, the use of MRI in radiotherapy planning for HNC is rapidly gaining popularity. MRI provides superior soft-tissue contrast in comparison with CT, allowing better definition of the tumour and OARs. The lack of additional radiation exposure is another attractive feature for intratreatment monitoring. In addition, advanced MRI techniques such as diffusion-weighted, dynamic contrast-enhanced and intrinsic susceptibility-weighted MRI techniques are capable of characterizing tumour biology further by providing quantitative functional parameters such as tissue cellularity, vascular permeability/perfusion and hypoxia. These functional parameters are known to have radiobiological relevance, which potentially could guide treatment adaptation based on their changes prior to or during radiotherapy. In this article, we first present an overview of the applications of anatomical MRI sequences in head and neck radiotherapy, followed by the potentials and limitations of functional MRI sequences in personalizing therapy.

INTRODUCTION

Radical radiotherapy (RT) is integral to the management of head and neck cancer (HNC) in both the primary and adjuvant settings. Advances in computer-assisted radiological techniques over the past two decades have in turn revolutionized radiotherapy planning. Development of advanced radiotherapy planning techniques such as intensity-modulated radiotherapy (IMRT) and volumetric-modulated arc therapy have allowed for better dose conformation to the tumour target and sparing of surrounding normal tissues. HNC was one of the first tumour sites where IMRT was widely implemented owing to a significant reduction in radiation-induced xerostomia in comparison with three-dimensional conformal planning.[1]

CT is currently the standard platform for radiotherapy planning. CT, however, provides a poor soft-tissue contrast, resulting in difficulty in identifying tumour and organs at risk (OARs) in the head and neck regions. On the contrary, MRI utilizes a strong magnetic field to provide high-resolution anatomical information by which blood vessels, masses and adjacent soft tissues are easily distinguishable. There is no increased risk of secondary malignancies with repetitive imaging, making MRI an attractive tool in the field of image-guided and adaptive radiotherapy.

The potential advantages of using MRI as a stand-alone radiotherapy planning platform have led to international collaboration to develop MR-Linac. MR-Linac aims to combine the two technologies in the MRI scanner and linear accelerator to address the current insufficiency in modern image-guided radiotherapy, *i.e.* to accurately define the tumour and tailor radiotherapy beams in real time. This would help eliminate the uncertainties related to patient setup, intrafraction and interfraction movements. However, there are several technical challenges with MR-Linac such as the lack of electron density data and the influence of magnetic field on radiotherapy dose distribution due to secondary electrons, which are currently being addressed during its development.

In addition, advanced MRI sequences, such as diffusion-weighted (DW), dynamic contrast-enhanced (DCE) and intrinsic susceptibility-weighted (ISW) sequences are capable of characterizing tumour biology further by providing quantitative functional parameters that are known to have radiobiological significance such as tissue cellularity, vascular perfusion/permeability and hypoxia. These sequences, also collectively referred to as functional MRI (F-MRI) in this article, are areas of ongoing research; but, there is increasing evidence to support the role of these F-MRI parameters as predictive and prognostic biomarkers.

In the first section of this article, we give an overview of the applications of anatomical MRI sequences in the management of HNC with specific focus on radiotherapy. For the purpose of this review, the term HNC refers primarily to squamous cell carcinoma, which accounts for over 90% of head and neck malignancies. Next, we elaborate on each F-MRI modality and discuss their potential utilities and limitations as imaging biomarkers to guide treatment individualization for HNC.

ANATOMICAL MRI SEQUENCES

Staging

MRI is increasingly used for defining the extent of tumour invasion into adjacent structures in HNC owing to its superior soft-tissue contrast. T_1 weighted images are generally considered the best for gross structural information, whereas T_2 weighted images distinguish abnormal pathology from surrounding tissues. In clinical practice, MRI is the imaging modality of choice for staging primary disease for nasopharyngeal and sinonasal tumours. It is also increasingly used to stage oropharyngeal (OP) cancer and detect cartilage invasion for laryngeal/hypopharyngeal cancer.[2]

MRI is also more reliable than CT at detecting the presence of pre-vertebral space invasion,[3] perineural spread[4] and retropharyngeal lymph node (LN) involvement,[5] which are all important factors for treatment decision-making. A study by Samuels et al[6] demonstrated retropharyngeal node involvement to be an independent poor prognostic feature, even for human papilloma virus (HPV)-driven OP cancer. Figure 1 shows an example of a metastatic retropharyngeal LN which was readily detectable on MRI, but not on CT.

Radiotherapy planning—tumour target and organ at risk delineation

Prior to the era of IMRT/volumetric-modulated arc therapy, head and neck radiotherapy planning has been historically based on compartmental volume, defined by anatomical boundaries. Consequently, radiation-induced toxicities were substantial with significant negative impact on patient quality of life. Advances in both diagnostic imaging and planning techniques have permitted a shift of practice towards volumetric contouring. This means that high-dose clinical target volume only includes the gross tumour volume (GTV) with a pre-determined margin for isotropic expansion, instead of the whole anatomical subsite. Importantly, no detrimental effect on locoregional control was observed with volumetric contouring.[7–9]

Several planning studies have underlined the benefit of incorporating MR images in head and neck radiotherapy planning with improvement of tumour delineation and reduction in interobserver variations compared with CT.[10–12] It also enables a more accurate delineation of neurological OARs such as the spinal cord, brain stem, optic chiasm and hippocampus, which is vital to avoid irreversible neurological sequelae. Nevertheless, the accuracy of MRI in this context is hugely dependent on the scanning position. Appropriate neck immobilization for planning MRI is necessary to reduce the risk of geographical miss, as deformable registration is unable to fully account for the differences in the position of the neck.[13,14] Acquiring MRI in neck immobilization requires deviation from standard protocol owing to inability to use the standard head coil. However, this can be overcome by using a combination of flex and spine coils.[15]

The majority of commonly used metallic implants, including dental objects, are MRI safe or conditional and can be imaged with MRI. However, these objects may cause local magnetic field

Figure 1. An example of axial T_2 weighted MR image showing contralateral retropharyngeal node involvement (b) (indicated by arrow) in a patient with left tonsillar squamous cell carcinoma, which was not readily visible on CT (a).

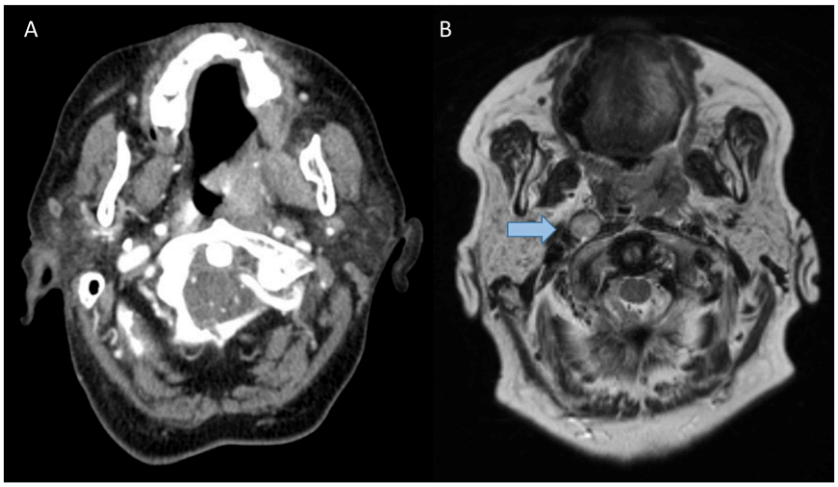

inhomogeneity, resulting in regional signal loss and "pile-ups" depending on the implant material and geometry.[16] In practice, these effects are often less problematic in comparison with CT streak artefact caused by beam hardening and photon starvation, thereby providing further advantage in radiotherapy planning. Furthermore, these artefacts can be greatly reduced for MRI by employing dedicated metal artefact reduction sequences, albeit at the expense of longer acquisition times.[17]

In addition, it is feasible to quantify the magnitude of tumour motion using cine-MRI. This enables an individualized internal margin to generate a planning target volume for each patient. Cine-MRI is acquired through continuous real-time imaging, which historically posed limitations with poor image quality in terms of spatial resolution and signal-to-noise ratio, but this has vastly improved with newer techniques.[18] A study assessing deglutition-induced organ motion with cine-MRI observed some tumour motion even in the absence of swallowing.[19] The use of a customized intraoral immobilization device could help minimize tongue movement and prevent swallowing,[20] but this service requires input from specialized orthodontics and is not widely available.

Radiotherapy delivery—adaptive approach

A patient anatomy changes throughout the course of radiotherapy, which may significantly alter the dose distribution to both planning target volume and OARs. This is a prominent issue for HNC owing to treatment-related weight loss. For example, parotids are known to shrink up to 30–40% of their original volume and tend to displace medially throughout the course of radiotherapy.[21,22] Adaptive radiotherapy studies with CT have already demonstrated the benefit of such an approach in reducing cumulative dose to normal tissues throughout the radiotherapy without compromising long-term outcome.[23–25]

MRI is naturally the imaging modality of choice for this approach owing to lack of additional radiation exposure and better soft-tissue contrast. Current imaging modalities available in the treatment room such as cone-beam CT or in-room CT provide limited soft-tissue contrast which precludes precise tumour tracking. One of the projected benefits with MR-Linac is that patients could be imaged daily to allow real-time online matching, dosimetric analysis and plan reoptimization if required. Moreover, GTV could be modified based on tumour response during radiotherapy, enabling further reduction in dose to adjacent organs (Figure 2). Efforts to develop automated OAR segmentation and rapid adaptive replanning are ongoing.

Functional MRI sequences

It is now evident that HNC represents a disease spectrum, which is divisible into different prognostic groups based on clinical variables such as clinical/radiological staging (Tumor, Node and Metastases), HPV status and smoking history. There is, therefore, a pressing need for a more personalized approach to treatment decision-making in order to optimize the balance between therapeutic efficacy and toxicity. However, biomarkers which could provide reliable information on the likely impact of a specific intervention at an early time point are required to guide treatment adaptation. F-MRI offers an attractive, non-invasive means to characterize the tumour biology by providing quantitative parameters with known radiobiological relevance. This has, in turn, led to a surge in the number of studies investigating the role of these parameters as imaging biomarkers for HNC over the past decade. In this section, we review the evidence and discuss the potential roles of these F-MRI sequences in the management of HNC.

Diffusion-weighted MRI

DW MRI utilizes the Brownian motion of water to assess tissue cellularity without the need of any exogenous contrast agent.

Figure 2. The coronal T_2 weighted MR images on the left are illustrating the early anatomical changes in primary gross tumour volume (GTV) observed following Week-1 and Week-2 radical chemoradiotherapy (CRT) in a patient with human papilloma virus-positive T3N0M0 left tonsillar squamous cell carcinoma. The axial image on the right is showing an overlay of co-registered MRIs between pre-treatment and Week-2 CRT for the same patient to illustrate the potential benefit of dose reduction to the pharyngeal constrictors and left parotid through GTV adaptation during radiotherapy with the shrinkage of the tumour away from these structures (filled contour—Week-2 CRT; dotted contour—pre-treatment).

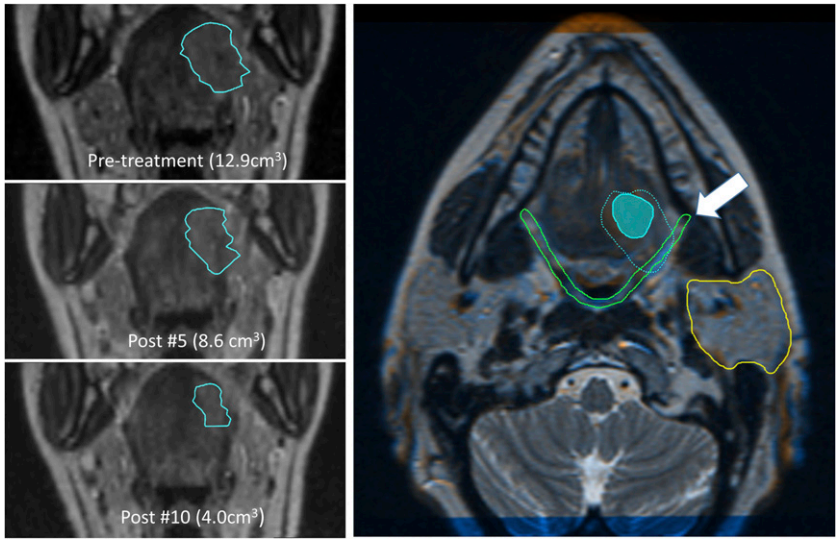

The movement of the tissue water molecules during the course of the diffusion-encoding gradients results in dephasing, depicted as signal loss. The signal loss is proportional to the amount of water molecule displacement and the duration of the diffusion-encoding gradients (*b*-value). The voxel-based signal loss can be quantified to produce maps of apparent diffusion coefficient (ADC), which is inversely correlated with tumour cellularity.[26]

DW sequences are increasingly incorporated in routine head and neck imaging owing to their additional values to anatomical sequences at diagnosing primary tumours (PTs), nodal involvement and detecting recurrences.[27] Vandecaveye et al[28] further reported the ability of DW MRI to differentiate between tumour and post-radiotherapy changes, thus enabling identification of residual tumour immediately after radiotherapy, in contrast to fludeoxyglucose-positron emission tomography (PET) which has a poor specificity in this situation.[29] The high contrast between tumour and surrounding tissues in heavily DW images has also raised the possibility to use this technique as an adjunct to guide GTV delineation. Nevertheless, this is hampered by geometric distortions which are pronounced in the head and neck region owing to the large magnetic field inhomogeneity caused by the tissue–air interface. A study by Schakel et al[30] found distortions up to 26 mm in the anteroposterior axis. This, however, can be minimized with dedicated acquisition and post-processing methods.[31,32] DW distortion in HNC was shown to be greatly compensated using reduced-distortion readout-segmented echoplanar imaging[33] and half-Fourier acquisition single-shot turbo spin echo (Figure 3). The latter, however, may not be optimal for qualitative tumour assessment owing to a low interobserver agreement for ADC values in lesions assessed with conventional echoplanar imaging *vs* half-Fourier acquisition single-shot turbo spin echo techniques.[34]

There are now much published data that support the ability of DW MRI to assist in the early prediction of treatment outcomes following chemoradiotherapy in HNC. Overall, there were conflicting results over the value of pre-treatment ADC at predicting response to treatment (Table 1). Five studies failed to distinguish patients with unfavourable disease based on pre-treatment ADC,[35–39] whereas six studies found high pre-treatment tumour ADC to be predictive of poor outcome following RT.[40–45] As illustrated in Table 1, there are heterogeneities between the studies in scanning protocol, analytical methods and measured clinical end points, which may be

Figure 3. A comparison of geometrical fidelity in head and neck diffusion-weighted (DW) images using conventional single-shot echoplanar imaging (SS-EPI) and the readout-segmented echoplanar imaging (RESOLVE). DW sequences were acquired in the axial plane, reformatted to the sagittal plane and overlaid with a T_2 weighted anatomical sequence. Geometrical distortion resulting in stretching or misslocation of anatomical signal can be observed in the SS-EPI sequence (inferior part of the spinal cord, cerebellum and position of lymph nodes). A high geometrical fidelity can be observed in the corresponding images acquired using RESOLVE (highlighted by the arrows).

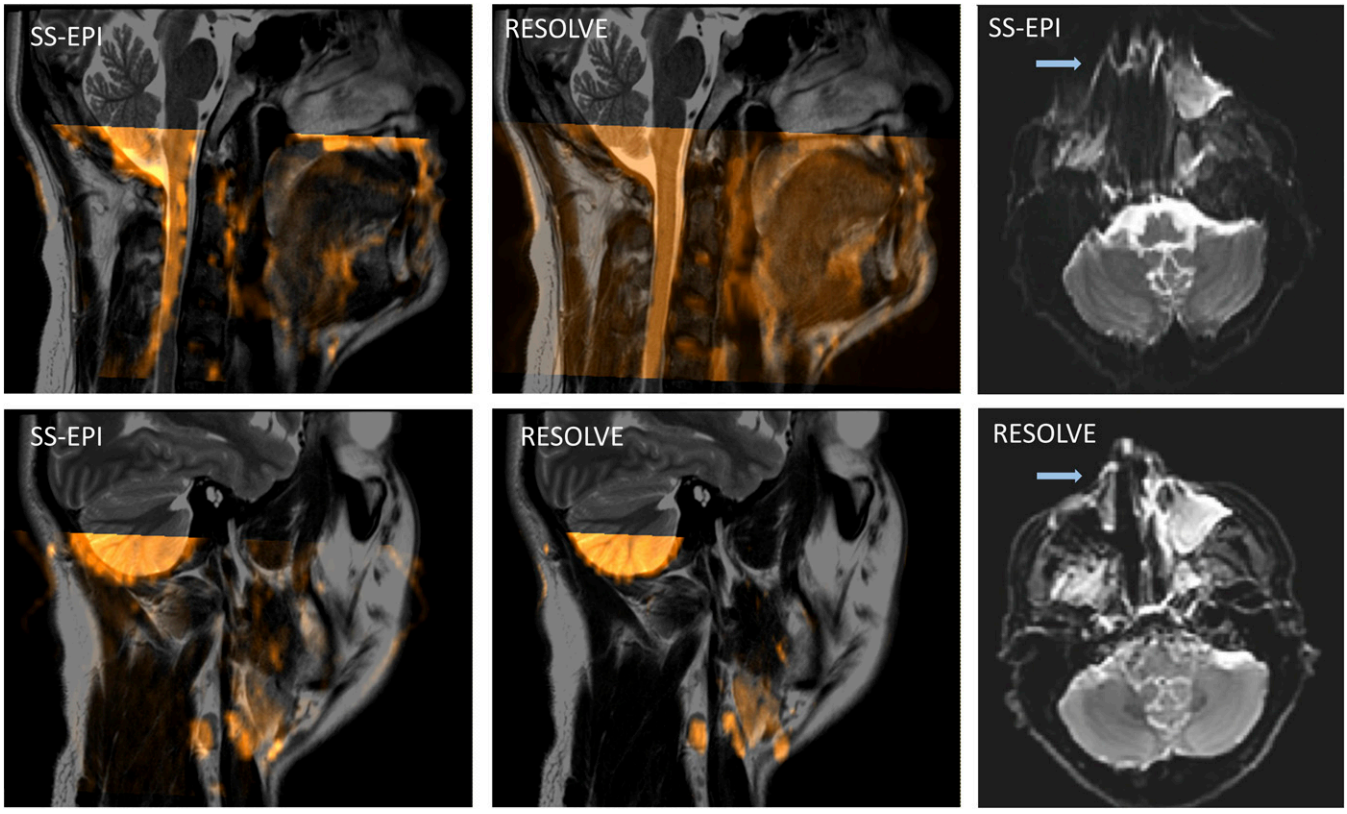

Table 1. Summary of diffusion-weighted (DW) MRI biomarker studies in head and neck cancer

Study	Design and treatment modalities	Scan time points	DW scanning protocol	Number of patients/ ROIs analyzed/ primary sites	End points (response criterion)	Results	Suggested ADC—thresholds
Kim et al[40] (2009)	Prospective, CRT	Pre-RT, Week 1 and Week 2 RT	1.5 T or 3.0 T; TR/TE: 4 s/89 ms ($b = 0$, 500, 1000 s mm^{-2})	33 patients (all Stage IV)/LNs only 66% oropharynx	CR *vs* PR based on clinical and pathological evidence post-CRT	CR group has a lower pre-treatment ADC	1.11×10^{-3} mm^2 s^{-1}
						CR group has a larger increase in ADC post-Week 1 (<0.01) and post-Week 2 RT (<0.05)	None
Kato et al[43] (2009)	Retrospective, neoadjuvant CRT, IC and RT	Pre-RT only	1.5 T; TR/TE: 5 s/70–72 ms ($b = 0$, 1000 s mm^{-2})	28 patients (Stage II–IV)/ both PTs and LNs 40% larynx/ hypopharynx	Tumour regression rate (RECIST) post-treatment	Inverse correlation of pre-treatment ADC with tumour regression rate (r = −0.384)	None
Vandecaveye et al[49] (2010)	Prospective, CRT and RT	Pre-RT, Week 2 and Week 4 RT	1.5 T; TR/TE: 7.1 s/84 ms ($b = 0$, 50, 100, 500, 750, 1000 s mm^{-2})	30 patients (Stage I–IV)/ both PTs and LNs 53% larynx/ hypopharynx	Locoregional control (median follow-up 2 years)	Lower increase in PTs and LNs ADC 2 and 4 weeks after treatment is associated with poor locoregional control at 2 years	PTs: 14% (Week 2) and 25% (Week 4) LNs: 14.6% (Week 2) and 19% (Week 4)
Hatakenaka et al[41] (2011)	Retrospective, CRT and RT	Pre-RT only	1.5 T; TR/TE: 3 s/73 ms ($b = 0$, 300, 1000 s mm^{-2})	38 patients (17 Stage ≥III)/ PTs only 60% hypopharynx/ larynx	LC *vs* local failure (median follow-up approximately 10 months)	LC group has a lower pre-treatment ADC	0.88×10^{-3} mm^2 s^{-1}
King et al[36] (2010)	Prospective, CRT and RT	Pre-RT, Week 2 RT and 6 weeks post-RT	1.5 T; TR/TE: 2 s/75 ms ($b = 0$, 100, 200, 300, 400, 500 s mm^{-2})	50 patients (Stage III–IV)/ single-slice ADC analysis of tumour with largest diameter >50% hypopharynx	Locoregional control (median follow-up 22 months)	No signal for pre-treatment ADC	N/A
						A fall in ADC during RT predicts for local failure	None
Ohnishi et al[48] (2011)	Retrospective, CRT and RT	Pre-RT only	1.5 T; TR/TE: 3 s/73 ms; ($b = 0$, 300, 1000 s mm^{-2})	32 patients, (Stage I–IV)/ PTs only 53% hypopharynx, 47% oropharynx	LC (median follow-up 15 months)	Low pre-treatment ADC predicts for LC	0.79×10^{-3} mm^2 s^{-1}
Berrak et al[38] (2011)	Retrospective, IC + CRT	Pre-IC and 3 weeks post-IC	1.5 or 3.0 T; TR/TE: 4 s/89 ms ($b = 0$, 500, 1000 s mm^{-2})	18 patients (Stage IV)/ LNs only 72% oropharynx	OS (median follow-up approximately 19 months)	No signal for pre-treatment ADC	N/A
						Alive—increase in ADC 22%, deceased—decrease in ADC 33%	None

(Continued)

Table 1. (Continued)

Study	Design and treatment modalities	Scan time points	DW scanning protocol	Number of patients/ ROIs analyzed/ primary sites	End points (response criterion)	Results	Suggested ADC—thresholds
Chawla et al[35] (2013)	Prospective, CRT and IC + CRT	Pre-RT only	1.5 T or 3.0 T; TR/TE: 4 s/89 ms ($b = 0$, 500, 1000 s mm^{-2})	24 patients (Stage III–IV)/ both PTs and LNs 94% oropharynx	Responders *vs* partial/ non-responders (median follow-up 23.7 months)	No signal from pre-treatment ADC alone (LN and PTs)	N/A
Matoba et al[37] (2014)	Prospective, CRT	Pre-RT and Week 3 RT	1.5 T; TR/TE: 4 s/68 ms ($b = 0$, 90, 800 s mm^{-2})	35 patients (Stage III–IV)/ both PTs and LNs 57% larynx/ hypopharynx	Locoregional control (median follow-up 30.8 months)	No signal from pre-treatment ADC	N/A
						A larger increase in PT ADC at Week 3 RT predicts for LC	24% increase in PT ADC
Ng et al[42] (2014)	Prospective, CRT	Pre-RT only	3.0 T; TR/TE: 8.2 s/84 ms ($b = 0$, 800 s mm^{-2})	69 patients (Stage III–IV)/ LNs only (largest) 53% oropharynx, 47% hypopharynx	3-year neck control (median follow-up 31 months)	Higher pre-treatment LN ADC is an independent predictor of poor neck control	1.14×10^{-3} mm^2 s^{-1}
Ng et al[45] (2016)	Prospective, CRT	Pre-RT only	3.0 T; TR/TE: 8.2 s/84 ms ($b = 0$, 800 s mm^{-2})	86 patients (Stage III–IV)/ both PTs and LNs 52% oropharynx, 48% hypopharynx	PFS and OS (median follow-up 36 months)	Lower LN ADC is an independent predictor of longer PFS but not OS	1.14×10^{-3} mm^2 s^{-1}
						PT ADC is not an independent predictor factor for PFS or OS	N/A
Wong et al[39] (2016)	Prospective, IC + CRT	Pre-IC, post-1st and 2nd cycle IC	1.5 T; TR/TE: 13 s/61 ms ($b = 50$, 400, 800 s mm^{-2})	20 patients (Stage III–IV)/ both PTs and LNs 90% oropharynx and 10% larynx/ hypopharynx	Complete remission 3 months post-CRT (median follow-up 14 months)	No signal from pre-treatment ADC or changes post-IC	N/A

ADC, apparent diffusion coefficient; CR, complete response; CRT, radical chemoradiotherapy; IC, induction chemotherapy; LC, local control; LN, lymph node; N/A, not applicable; OS, overall survival; PFS, progression-free survival; PR, partial response; PT, primary tumour; ROI, region of interest; RT, radical radiotherapy; TE, echo time; TR, repetition time.

accountable for the discrepancy in their findings. Some investigators used different magnetic field strengths (1.5 T or 3.0 T) even within the same study and the number of *b*-values used ranged from 2 to 5. Whilst almost all studies excluded apparent tumour necrosis from ADC calculation, there is a lack of consensus on the analytical methods: some studies only chose the tumour with the largest diameter (primary or LN), whereas others analyzed them in isolation. However, the pre-treatment ADC thresholds suggested by the positive studies appear to be fairly concordant with primary ADC $<0.79–0.88 \times 10^{-3}$ mm^2 s^{-1} and nodal ADC $<1.11–1.14 \times 10^{-3}$ mm^2 s^{-1} to be predictive of favourable outcome following radiotherapy.[40,41,44,45] A contradictory result by Nakajo et al,[46] where they found patients with low pre-treatment primary ADC $<0.88 \times 10^{-3}$ mm^2 s^{-1} to have an unfavourable 2-year outcome, somewhat highlighted the potential negative influence of including inhomogeneous tumour sites and treatment modalities in the study findings: 54% patients undergoing primary surgery instead of radiotherapy, with higher recurrence rate in patients undergoing surgery.

Another noteworthy observation by Wong et al[39] is that HPV-positive OP tumours in patients who achieved complete remission following chemoradiotherapy exhibited a wide range of pre-treatment ADC ($0.9–1.54 \times 10^{-3}\,mm^2\,s^{-1}$), thereby undermining its predictive value. HPV-positive OP cancer (tonsil and base of tongue) is known to exhibit unique histopathological features such as indistinct cell borders and comedo necrosis, unlike other subsites or HPV-negative disease.[47,48] These features may have contributed to the high ADC in some HPV-positive tumours but, importantly, they do not have the same negative biological impact on treatment outcome as on a patient who is HPV negative.[48] The potential impact of HPV status on ADC measurements in OP cancer has not been explored in other published studies; hence, caution should be exercised when interpreting pre-treatment ADC alone.

Whilst the value of pre-treatment ADC remains unclear, treatment-induced changes of ADC during radiotherapy have been more consistently demonstrated in several clinical studies.[36,37,40,49] The cumulative results suggest that tumours that show a lower increase or even a decrease in ADC 1–4 weeks into radiotherapy (ΔADC <14–24%) are more likely to fail treatment. It is speculated that tumours with a good treatment response show a higher frequency of apoptosis or necrosis earlier in the course of treatment than those with a poor response. Thus, the ADC tends to increase in responding tumours because of the presence of fewer barrier structures to the movement of tissue water such as cell membranes. The optimal timing for early intratreatment assessment using DW MRI, however, still needs to be established (between Week 1 and Week 4 of RT), as development of mature scar tissues may "falsely" decrease ADC in responders.[50]

The majority of published studies have calculated mean or median ADC from defined regions of interest to quantitate the observed differences in DW MRI between patients at baseline and during treatment. More sophisticated analyses of DW MRI data are possible and may enable DW MRI to be used as a more sensitive and specific biomarker to provide an early prediction of response to chemoradiotherapy. Galban et al[51] described a voxelwise approach to the evaluation of ADC changes during treatment that involves the calculation of parametric response maps (PRM) in 12 patients. This approach uses registered baseline and intratreatment ADC maps to calculate regional tumour response and they concluded that PRM may be more sensitive to cellular changes than measurements of the change in the mean ADC over whole regions of interest. One lingering uncertainty, however, is how well deformable image registration accounts for volumetric or positional changes in tumour between the scanning time points to allow confident per-voxel analysis. Moreover, deformable image registration itself remains a matter of research with lack of clinical validation. Further studies on larger numbers of patients are, therefore, required.

Dynamic contrast-enhanced MRI

DCE MRI assesses changes in signal intensity following the injection of a paramagnetic contrast agent, *e.g.* gadolinium that shortens the longitudinal relaxation time (T_1). This leads to increased signal intensity in perfused tissue regions in T_1 weighted images. The temporal changes in signal intensity obtained by DCE MRI are related to the underlying permeability and perfusion of tumour microenvironment, all of which are known to influence treatment response. The gadolinium concentration–time curve can also be fitted to a two-compartment pharmacokinetic model to yield various kinetic and volumetric parameters such as the transfer coefficient from plasma to the interstitial space (K_{trans}), the extracellular extravascular volume fraction (V_e) and plasma volume fraction (V_p).

Enhancement patterns of DCE MRI have shown correlations with malignancy,[52] angiogenesis,[53] proliferation[54] and hypoxia.[55,56] One of the first studies to evaluate the relationship between tumour perfusion and local control (LC) using DCE MRI in patients with HNC was published by Hoskin et al.[57] 13 patients underwent DCE MRI before and on completion of accelerated radiotherapy. LC was found to be related to maximum tumour enhancement following radiotherapy and the difference in time taken to reach maximum tumour enhancement pre- and post-radiotherapy. These results suggested that tumours with lower perfusion at the end of radiotherapy were most sensitive to treatment and those with greater tumour enhancement were likely to fail locally.

Since then, several other groups have evaluated the ability of pre-treatment DCE parameters to provide prognostic information for patients with HNC undergoing radical chemoradiotherapy (CRT). These studies have been summarized in two systematic reviews published in recent years.[58,59] The most commonly reported pre-treatment DCE parameters with predictive or prognostic value are K_{trans}, followed by V_e and V_p. Two earlier clinical studies have shown low pre-treatment nodal tumour K_{trans} to be correlated with poor locoregional control and disease-free survival.[60,61] No threshold was suggested, but non-responders in both studies have an average K_{trans} value of $0.15–0.21\,min^{-1}$. However, one of the larger study to date by Shukla-Dave et al[62] reported that it was the skewness rather than the mean value of nodal tumour K_{trans} which was the strongest predictor of progression-free survival (PFS). The authors therefore recommended calculation of skewness to be a better measure of tumour heterogeneity, but did not indicate whether a positive or negative skew predicted for a better outcome.

Another large multimodality, parametric functional imaging study of 69 patients by Ng et al[42] reported low pre-treatment nodal V_e (<0.23) to be an independent poor prognostic factor for 3-year neck control for patients undergoing CRT. This is one of the first study reported in HNC to incorporate multimodality functional imaging in fluorine-18 fludeoxyglucose-PET/CT, DCE and DW MRI, given emerging evidence from correlation studies that these modalities provide different, but complementary biological tumour information,[63] thereby improving predictive power. It is noteworthy that none of these studies reported DCE parameters for PTs and this may be related to technical difficulties, *e.g.* motion caused by swallowing or susceptibility artefacts. A more recent study by King et al[64] in 49 patients assessed the predictive value of pre-treatment DCE

parameters in both primary and nodal tumours but failed to show any correlation with response to chemoradiotherapy. Ng et al[45] also provided an update on their previous study after recruiting additional 17 patients and including PT in analysis. This showed a similar result, *i.e.* low pre-treatment nodal V_e independently predicted for shorter PFS and overall survival (OS).

It is possible to conclude from the cumulative results shown above that pre-treatment DCE-derived K_{trans} or V_e in LNs could predict for outcome following radiotherapy in HNC. However, it is impossible to deduce which are the optimal pre-treatment parameters and the inconsistencies in the reported results are invariably attributable to the differences in DCE scanning protocols, pharmacokinetic models and arterial input function used. For example, there are up to four methodologies available to estimate arterial input function, *e.g.* population averaged,[65] reference tissue based,[66] contrast concentration in adjacent arteries[67] and independent component analysis.[68] Consequently, large collective efforts are required to optimize and standardize DCE protocols for future studies.

In contrast, there is a paucity of data on the role of intratreatment DCE MRI to assess and predict response to radiotherapy. The number of patients in these studies are very small ($n < 15$), precluding any definitive conclusion or clinical translation. One of the first study by Cao et al[69] reported an increase of blood volume (BV) in PT 2 weeks into chemoradiotherapy to be associated with LC. Wang et al[70] subsequently reported on a cluster analysis method to identify biologically relevant tumour subvolumes using DCE MRI. The sizes of the cluster analysis-defined tumour subvolumes with low BV, before and during Week-2 radiotherapy, were significantly greater in the patients with local treatment failure (LF) than that in those with LC. Whilst the total PT volumes were reduced from baseline to Week 2 to a similar extent for both patients with LF and LC, the percentage decreases in the subvolumes of the PTs with low BV in the same time interval were significantly smaller for the patients with LF than that for those with LC ($p < 0.05$).[70] This illustrates the potential utility of DCE parameters to identify a biological target volume for radiotherapy dose escalation and using it to monitor response.

Baer et al[71] investigated the feasibility of using PRM of DCE MRI to predict survival following CRT in 10 patients. They found that the reduction in K_{trans} per voxel measured through PRM after 2 weeks of radiotherapy was a better predictor of OS in comparison with the whole tumour mean or median signal changes. Similar to the DW PRM study, this needs to be validated with more patients. The authors themselves acknowledged that the process to analyze PRM is complex and requires special attention during delineation owing to limitations in image resolution.

Intrinsic susceptibility-weighted MRI

Hypoxia is a well-recognized factor of resistance to chemotherapy and radiotherapy in HNC. A meta-analysis has demonstrated hypoxia modification to be a valid therapeutic strategy;[72] thus, a non-invasive mean to detect tumour hypoxia is highly desirable to guide identification of patients who are likely to benefit from such a strategy. PET-based techniques using tracers such as fluorine-18 fluoromisonidazole are currently the most widely studied functional imaging to characterize hypoxia in HNC. However, these PET techniques are expensive, time consuming and suffer from a poor spatio-temporal resolution and signal-to-noise ratio.[73]

An alternative hypoxia-specific imaging technique is ISW MRI, also known as blood oxygen level-dependent MRI. It exploits the paramagnetic properties of deoxyhaemoglobin in erythrocytes to create contrast. Essentially, deoxyhaemoglobin creates magnetic susceptibility perturbations around blood vessels and the transverse MR relaxation rate R_2^* ($R_2^* = 1/T_2^*$) of water in blood and the surrounding tissues increases in proportion to tissue deoxyhaemoglobin concentration. Because oxygenation of haemoglobin is proportional to arterial blood polarographic oxygen levels, tumour R_2^* is a sensitive index of tissue oxygenation and a surrogate marker of hypoxia.

ISW MRI has been typically performed by measuring changes in R_2^* with hyperoxic gas challenge such as carbogen. Clinical studies conducted in patients with HNC have consistently demonstrated that the tumour R_2^* decreases following inhalation of hyperoxic gas, indicative of improved blood oxygenation which may further increase the radiosensitivity.[74,75] The use of hyperoxic gas breathing in clinical practice remains limited owing to added complexity and side effects such as breathlessness. However, there are now emerging data that suggest that useful information may still be obtained from ISW MRI, even in the absence of oxygen challenge. A study in cervical cancer by Li et al[76] was one of the first studies to demonstrate the ability of using baseline tumour R_2^* alone to predict response to chemoradiotherapy: responders had a lower baseline R_2^* than non-responders. This study also found baseline R_2^* to be an independent prognostic factor for PFS and OS. However, these results are yet to be replicated in other tumour sites.

A study by Panek et al[77] has demonstrated tumour R_2^* measurement to be a sensitive and reproducible quantitative imaging technique in detecting clinically relevant changes in tumour oxygenation for HNC. However, reliable interpretation of R_2^* as a stand-alone parameter is not possible without additional information such as tumour BV.[77] This is supported by other observations that hypoxic tumours with high blood flow had high R_2^*,[78] whereas hypoxic tumours with low BV were found to have low R_2^* instead.[79] Serial weekly changes in R_2^* alone throughout chemoradiotherapy in patients with HNC also did not appear to show any clear pattern.[80] Therefore, a better understanding of how to interpret R_2^* measurements with BV needs to be ascertained to improve its performance as an imaging biomarker.

Challenges with integration of functional MRI into clinical practice

Whilst there is little doubt that F-MRI can provide predictive and prognostic information for HNC, its integration into clinical practice remains limited. One of the main reasons is the lack of consensus of optimal modalities, scanning protocols and analytical methodologies, leading to discrepancy in the reported results (as described above). This is partly due to the constant

Figure 4. A schematic summarizing the potential applications of MRI in the management, radiotherapy planning and delivery of head and neck cancer. BTV, biological target volume; DCE, dynamic contrast-enhanced; DW, diffusion-weighted; F-MRI, functional MRI; HPV, human papilloma virus; ISW, intrinsic susceptibility-weighted; OAR, organ at risk; RT, radical radiotherapy.

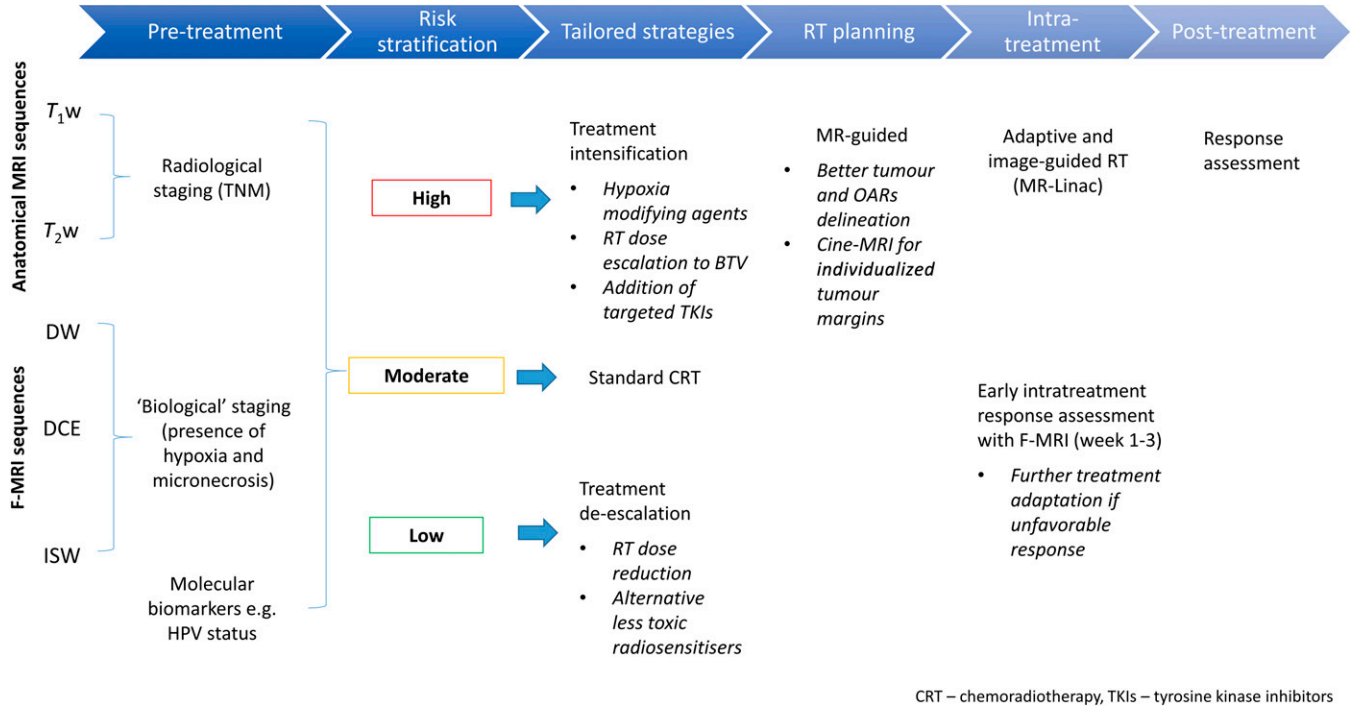

evolution of machinery and acquisition techniques over the years. Consequently, a meta-analysis of F-MRI studies is not possible for the same reason. Efforts to standardize these protocols for clinical trials are under way and may be further facilitated through collaboration between MR-Linac consortiums.

Another important issue to consider is that physiological parameters, such as perfusion and oxygenation, are dynamic and potentially unstable parameters that may fluctuate significantly in the absence of therapy. Only limited data exist on the stability of F-MRI parameters in patients with cancer prior to treatment and there are no data on this aspect that are specific to patients with HNC receiving primary CRT. However, two studies in patients with a variety of cancers enrolled in Phase 1 clinical drug trials do provide some reassuring data on the reproducibility of F-MRI parameters. Koh et al[81] found ADC measurements from DW-MRI to be highly reproducible, with a coefficient of repeatability of 13.3%. Messiou et al[82] also reported the intrapatient coefficients of variation (CVs) for all DCE-derived parameters to be within the range of 8–30%, except for V_p.[82] The most reproducible DCE-derived parameters were the enhancing fraction (CV = 8.6%), followed by K_{trans} (CV = 13.9%) and initial area under the time-concentration curve over 60 seconds (CV = 15.5%). The stability of these parameters in HNC need to be established further prior to clinical implementation.

Furthermore, integration of F-MRI into radiotherapy treatment planning requires special attention in terms of image quality and geometrical accuracy, which means that image acquisition with immobilization in the radiotherapy treatment position is essential. This approach was lacking in most earlier F-MRI studies, which precluded the analysis of PT owing to gross motion artefact. Consequently, tolerability may be an issue for some patients owing to the additional discomfort with immobilization and scanning time required in comparison with standard anatomical MRI. Considerations should also be given to the potential pressure on the hospital resources, *e.g.* time on scanners and additional expertise required to process F-MRI images.

CONCLUSION

Anatomical and functional imaging capabilities offered by MRI provide potential opportunities to optimize radiotherapy strategies for HNC through improved target delineation, high-risk disease subvolume identification, early intratreatment monitoring and adaptation based on response (Figure 4). Based on current evidence, baseline tumour vascular permeability/hypoxia and early cell apoptosis during radiotherapy, as measured by DCE and DW MRI, respectively, appear to be the most promising biomarkers to predict radiotherapy outcome and tailor treatment strategies for HNC. The studies conducted to date have laid a solid foundation for the exciting prospect of integrating functional imaging into MR-Linac in the future. This added dimension will further enhance the appeal of using MRI as a single platform for radiotherapy planning and delivery in HNC. However, an important next step to bridge the translational gaps for F-MRI is a collective effort to determine the optimal methodology to allow standardization and perform clinical validation through a large multicentre study.

FUNDING

The authors of this article are supported by the Cancer Research UK head and neck programme grant C7224/A13407.

REFERENCES

1. Nutting CM, Morden JP, Harrington KJ, Urbano TG, Bhide SA, Clark C, et al. Parotid-sparing intensity modulated *versus* conventional radiotherapy in head and neck cancer (PARSPORT): a phase 3 multicentre randomised controlled trial. *Lancet Oncol* 2011; **12**: 127–36. doi: https://doi.org/10.1016/S1470-2045(10)70290-4
2. Wippold FJ. Head and neck imaging: the role of CT and MRI. *J Magn Reson Imaging* 2007; **25**: 453–65. doi: https://doi.org/10.1002/jmri.20838
3. Hsu WC, Loevner LA, Karpati R, Ahmed T, Mong A, Battineni ML, et al. Accuracy of magnetic resonance imaging in predicting absence of fixation of head and neck cancer to the prevertebral space. *Head Neck* 2005; **27**: 95–100. doi: https://doi.org/10.1002/hed.20128
4. Baulch J, Gandhi M, Sommerville J, Panizza B. 3T MRI evaluation of large nerve perineural spread of head and neck cancers. *J Med Imaging Radiat Oncol* 2015; **59**: 578–85. doi: https://doi.org/10.1111/1754-9485.12338
5. Kato H, Kanematsu M, Watanabe H, Mizuta K, Aoki M. Metastatic retropharyngeal lymph nodes: comparison of CT and MR imaging for diagnostic accuracy. *Eur J Radiol* 2014; **83**: 1157–62. doi: https://doi.org/10.1016/j.ejrad.2014.02.027
6. Samuels SE, Vainshtein J, Spector ME, Ibrahim M, McHugh JB, Tao Y, et al. Impact of retropharyngeal adenopathy on distant control and survival in HPV-related oropharyngeal cancer treated with chemoradiotherapy. *Radiother Oncol* 2015; **116**: 75–81. doi: https://doi.org/10.1016/j.radonc.2015.06.006
7. Loo SW, Geropantas K, Wilson P, Martin WMC, Roques TW. Target volume definition for intensity-modulated radiotherapy after induction chemotherapy and patterns of treatment failure after sequential chemo-radiotherapy in locoregionally advanced oropharyngeal squamous cell carcinoma. *Clin Oncol (R Coll Radiol)* 2013; **25**: 162–70. doi: https://doi.org/10.1016/j.clon.2012.07.015
8. Sanguineti G, Gunn GB, Endres EJ, Chaljub G, Cheruvu P, Parker B. Patterns of locoregional failure after exclusive IMRT for oropharyngeal carcinoma. *Int J Radiat Oncol Biol Phys* 2008; **72**: 737–46. doi: https://doi.org/10.1016/j.ijrobp.2008.01.027
9. Daly ME, Le QT, Maxim PG, Loo BW, Kaplan MJ, Fischbein NJ, et al. Intensity-modulated radiotherapy in the treatment of oropharyngeal cancer: clinical outcomes and patterns of failure. *Int J Radiat Oncol Biol Phys* 2010; **76**: 1339–46. doi: https://doi.org/10.1016/j.ijrobp.2009.04.006
10. Ahmed M, Schmidt M, Sohaib A, Kong C, Burke K, Richardson C, et al. The value of magnetic resonance imaging in target volume delineation of base of tongue tumours—a study using flexible surface coils. *Radiother Oncol* 2010; **94**: 161–7. doi: https://doi.org/10.1016/j.radonc.2009.12.021
11. Emami B, Sethi A, Petruzzelli GJ. Influence of MRI on target volume delineation and IMRT planning in nasopharyngeal carcinoma. *Int J Radiat Oncol Biol Phys* 2003; **57**: 481–8. doi: https://doi.org/10.1016/S0360-3016(03)00570-4
12. Rasch C, Keus R, Pameijer FA, Koops W, de Ru V, Muller S, et al. The potential impact of CT-MRI matching on tumor volume delineation in advanced head and neck cancer. *Int J Radiat Oncol Biol Phys* 1997; **39**: 841–8. doi: https://doi.org/10.1016/S0360-3016(97)00465-3
13. Fortunati V, Verhaart RF, Verduijn GM, van der Lugt A, Angeloni F, Niessen WJ, et al. MRI integration into treatment planning of head and neck tumors: can patient immobilization be avoided? *Radiother Oncol* 2015; **115**: 191–4. doi: https://doi.org/10.1016/j.radonc.2015.03.021
14. Hanvey S, McJury M, Tho LM, Glegg M, Thomson M, Grose D, et al. The influence of MRI scan position on patients with oropharyngeal cancer undergoing radical radiotherapy. *Radiat Oncol* 2013; **8**: 129. doi: https://doi.org/10.1186/1748-717X-8-129
15. Welsh L, Panek R, McQuaid D, Dunlop A, Schmidt M, Riddell A, et al. Prospective, longitudinal, multi-modal functional imaging for radical chemo-IMRT treatment of locally advanced head and neck cancer: the INSIGHT study. *Radiat Oncol* 2015; **10**: 112. doi: https://doi.org/10.1186/s13014-015-0415-7
16. Clayman DA, Murakami ME, Vines FS. Compatibility of cervical spine braces with MR imaging: a study of nine nonferrous devices. *AJNR Am J Neuroradiol* 1990; **11**: 385–90.
17. Schmidt MA, Panek R, Colgan R, Hughes J, Sohaib A, Saran F, et al. Slice encoding for metal artefact correction in magnetic resonance imaging examinations for radiotherapy planning. *Radiother Oncol* 2016; **120**: 356–62. doi: https://doi.org/10.1016/j.radonc.2016.05.004
18. Uecker M, Zhang S, Voit D, Karaus A, Merboldt KD, Frahm J. Real-time MRI at a resolution of 20 ms. *NMR Biomed* 2010; **23**: 986–94. doi: https://doi.org/10.1002/nbm.1585
19. Paulson ES, Bradley JA, Wang D, Ahunbay EE, Schultz C, Li XA. Internal margin assessment using cine MRI analysis of deglutition in head and neck cancer radiotherapy. *Med Phys* 2011; **38**: 1740–9. doi: https://doi.org/10.1118/1.3560418
20. Ding Y, Mohamed ASR, Yang J, Colen RR, Frank SJ, Wang J, et al. Prospective observer and software-based assessment of magnetic resonance imaging quality in head and neck cancer: should standard positioning and immobilization be required for radiation therapy applications? *Pract Radiat Oncol* 2015; **5**: e299–308. doi: https://doi.org/10.1016/j.prro.2014.11.003
21. Barker JL, Garden AS, Ang KK, O'Daniel JC, Wang H, Court LE, et al. Quantification of volumetric and geometric changes occurring during fractionated radiotherapy for head-and-neck cancer using an integrated CT/linear accelerator system. *Int J Radiat Oncol Biol Phys* 2004; **59**: 960–70. doi: https://doi.org/10.1016/j.ijrobp.2003.12.024
22. Bhide SA, Davies M, Burke K, McNair HA, Hansen V, Barbachano Y, et al. Weekly volume and dosimetric changes during chemoradiotherapy with intensity-modulated radiation therapy for head and neck cancer: a prospective observational study. *Int J Radiat Oncol Biol Phys* 2010; **76**: 1360–8. doi: https://doi.org/10.1016/j.ijrobp.2009.04.005
23. Schwartz DL, Garden AS, Thomas J, Chen Y, Zhang Y, Lewin J, et al. Adaptive radiotherapy for head-and-neck cancer: initial clinical outcomes from a prospective trial. *Int J Radiat Oncol Biol Phys* 2012; **83**: 986–93. doi: https://doi.org/10.1016/j.ijrobp.2011.08.017
24. Kataria T, Gupta D, Goyal S, Bisht SS, Basu T, Abhishek A, et al. Clinical outcomes of adaptive radiotherapy in head and neck cancers. *Br J Radiol* 2016; **89**: 20160085–6. doi: https://doi.org/10.1259/bjr.20160085
25. Olteanu LA, Berwouts D, Madani I, De Gersem W, Vercauteren T, Duprez F, et al. Comparative dosimetry of three-phase adaptive and non-adaptive dose-painting IMRT for head-and-neck cancer. *Radiother Oncol* 2014; **111**: 348–53. doi: https://doi.org/10.1016/j.radonc.2014.02.017
26. Chen L, Liu M, Bao J, Xia Y, Zhang J, Zhang L, et al. The correlation between apparent diffusion coefficient and tumor cellularity in patients: a meta-analysis. *PLoS One* 2013; **8**:

e79008–9. doi: https://doi.org/10.1371/journal.pone.0079008
27. Chawla S, Kim S, Wang S, Poptani H. Diffusion-weighted imaging in head and neck cancers. *Future Oncol* 2009; **5**: 959–75. doi: https://doi.org/10.2217/fon.09.77
28. Vandecaveye V, De Keyzer F. Evaluation of the larynx for tumour recurrence by diffusion-weighted MRI after radiotherapy: initial experience in four cases. *Br J Radiol* 2014; **79**: 681–7.
29. Moeller BJ, Rana V, Cannon BA, Williams MD, Sturgis EM, Ginsberg LE, et al. Prospective risk-adjusted [18F]fluorodeoxyglucose positron emission tomography and computed tomography assessment of radiation response in head and neck cancer. *J Clin Oncol* 2009; **27**: 2509–15. doi: https://doi.org/10.1200/JCO.2008.19.3300
30. Schakel T, Hoogduin JM, Terhaard CH, Philippens ME. Diffusion weighted MRI in head-and-neck cancer: geometrical accuracy. *Radiother Oncol* 2013; **109**: 394–7. doi: https://doi.org/10.1016/j.radonc.2013.10.004
31. Jezzard P, Balaban RS. Correction for geometric distortion in echo planar images from B0 field variations. *Magn Reson Med* 1995; **34**: 65–73. doi: https://doi.org/10.1002/mrm.1910340111
32. Wu M, Chang LC, Walker L, Lemaitre H, Barnett AS, Marenco S, et al. Comparison of EPI distortion correction methods in diffusion tensor MRI using a novel framework. *Med Image Comput Comput Assist Interv* 2008; **11**: 321–9.
33. Koyasu S, Iima M, Umeoka S, Morisawa N, Porter DA, Ito J, et al. The clinical utility of reduced-distortion readout-segmented echo-planar imaging in the head and neck region: initial experience. *Eur Radiol* 2014; **24**: 3088–96. doi: https://doi.org/10.1007/s00330-014-3369-5
34. Schouten CS, de Bree R, van der Putten L, Noij DP, Hoekstra OS, Comans EFI, et al. Diffusion-weighted EPI- and HASTE-MRI and 18F-FDG-PET-CT early during chemoradiotherapy in advanced head and neck cancer. *Quant Imaging Med Surg* 2014; **4**: 239–50. doi: https://doi.org/10.3978/j.issn.2223-4292.2014.07.15
35. Chawla S, Kim S, Dougherty L, Wang S, Loevner LA, Quon H, et al. Pretreatment diffusion-weighted and dynamic contrast-enhanced MRI for prediction of local treatment response in squamous cell carcinomas of the head and neck. *AJNR Am J Neuroradiol* 2013; **200**: 35–43.
36. King AD, Mo FK, Yu KH, Yeung DK, Zhou H, Bhatia KS, et al. Squamous cell carcinoma of the head and neck: diffusion-weighted MR imaging for prediction and monitoring of treatment response. *Eur Radiol* 2010; **20**: 2213–20. doi: https://doi.org/10.1007/s00330-010-1769-8
37. Matoba M, Tuji H, Shimode Y, Toyoda I, Kuginuki Y, Miwa K, et al. Fractional change in apparent diffusion coefficient as an imaging biomarker for predicting treatment response in head and neck cancer treated with chemoradiotherapy. *AJNR Am J Neuroradiol* 2014; **35**: 379–85. doi: https://doi.org/10.3174/ajnr.A3706
38. Berrak S, Chawla S, Kim S, Quon H, Sherman E, Loevner LA, et al. Diffusion weighted imaging in predicting progression free survival in patients with squamous cell carcinomas of the head and neck treated with induction chemotherapy. *Acad Radiol* 2011; **18**: 1225–32. doi: https://doi.org/10.1016/j.acra.2011.06.009
39. Wong KH, Panek R, Welsh L, McQuaid D, Dunlop A, Riddell A, et al. The predictive value of early assessment after 1 cycle of induction chemotherapy with 18F-FDG PET/CT and diffusion-weighted MRI for response to radical chemoradiotherapy in head and neck squamous cell carcinoma. *J Nucl Med* 2016; **57**: 1843–50. doi: https://doi.org/10.2967/jnumed.116.174433
40. Kim S, Loevner L, Quon H, Sherman E, Weinstein G, Kilger A, et al. Diffusion-weighted magnetic resonance imaging for predicting and detecting early response to chemoradiation therapy of squamous cell carcinomas of the head and neck. *Clin Cancer Res* 2009; **15**: 986–94. doi: https://doi.org/10.1158/1078-0432.CCR-08-1287
41. Hatakenaka M, Nakamura K, Yabuuchi H, Shioyama Y, Matsuo Y, Ohnishi K, et al. Pretreatment apparent diffusion coefficient of the primary lesion correlates with local failure in head-and-neck cancer treated with chemoradiotherapy or radiotherapy. *Int J Radiat Oncol Biol Phys* 2011; **81**: 339–45. doi: https://doi.org/10.1016/j.ijrobp.2010.05.051
42. Ng SH, Lin CY, Chan SC, Lin YC, Yen TC, Liao CT, et al. Clinical utility of multimodality imaging with dynamic contrast-enhanced MRI, diffusion-weighted MRI, and 18F-FDG PET/CT for the prediction of neck control in oropharyngeal or hypopharyngeal squamous cell carcinoma treated with chemoradiation. *PLoS One* 2014; **9**: e115933. doi: https://doi.org/10.1371/journal.pone.0115933
43. Kato H, Kanematsu M, Tanaka O, Mizuta K, Aoki M, Shibata T, et al. Head and neck squamous cell carcinoma: usefulness of diffusion-weighted MR imaging in the prediction of a neoadjuvant therapeutic effect. *Eur Radiol* 2009; **19**: 103–9. doi: https://doi.org/10.1007/s00330-008-1108-5
44. Ohnishi K, Shioyama Y, Hatakenaka M, Nakamura K, ABE K, Yoshiura T, et al. Prediction of local failures with a combination of pretreatment tumor volume and apparent diffusion coefficient in patients treated with definitive radiotherapy for hypopharyngeal or oropharyngeal squamous cell carcinoma. *J Radiat Res* 2011; **52**: 522–30. doi: https://doi.org/10.1269/jrr.10178
45. Ng SH, Lin CY, Chan SC, Lin YC, Yen TC, Liao CT, et al. Dynamic contrast-enhanced MRI, diffusion-weighted MRI and 18F-FDG PET/CT for the prediction of survival in oropharyngeal or hypopharyngeal squamous cell carcinoma treated with chemoradiation. *Eur Radiol* 2016; **26**: 4162–72. doi: https://doi.org/10.1007/s00330-016-4276-8
46. Nakajo M, Nakajo M, Kajiya Y, Tani A, Kamiyama T, Yonekura R, et al. FDG PET/CT and diffusion-weighted imaging of head and neck squamous cell carcinoma: comparison of prognostic significance between primary tumor standardized uptake value and apparent diffusion coefficient. *Clin Nucl Med* 2012; **37**: 475–80. doi: https://doi.org/10.1097/RLU.0b013e318248524a
47. El-Mofty SK, Lu DW. Prevalence of human papillomavirus type 16 DNA in squamous cell carcinoma of the palatine tonsil, and not the oral cavity, in young patients: a distinct clinicopathologic and molecular disease entity. *Am J Surg Pathol* 2003; **27**: 1463–70.
48. Chernock RD, El-Mofty SK, Thorstad WL, Parvin CA, Lewis JS. HPV-related nonkeratinizing squamous cell carcinoma of the oropharynx: utility of microscopic features in predicting patient outcome. *Head Neck Pathol* 2009; **3**: 186–94. doi: https://doi.org/10.1007/s12105-009-0126-1
49. Vandecaveye V, Dirix P, De Keyzer F, de Beeck KO, Vander Poorten V, Roebben I, et al. Predictive value of diffusion-weighted magnetic resonance imaging during chemoradiotherapy for head and neck squamous cell carcinoma. *Eur Radiol* 2010; **20**: 1703–14. doi: https://doi.org/10.1007/s00330-010-1734-6
50. Padhani AR, Koh DM, Collins DJ. Whole-body diffusion-weighted MR imaging in cancer: current status and research directions. *Radiology* 2011; **261**: 700–18. doi: https://doi.org/10.1148/radiol.11110474
51. Galban CJ, Mukherji SK, Chenevert TL, Meyer CR. A feasibility study of parametric response map analysis of diffusion-weighted magnetic resonance imaging scans of head and neck cancer patients for providing early detection of therapeutic efficacy. *Transl Oncol* 2009; **2**: 184–90.
52. Hulka CA, Smith BL, Sgroi DC, Tan L, Edmister WB, Semple JP, et al. Benign and malignant breast lesions: differentiation with

echo-planar MR imaging. *Radiology* 1995; **197**: 33–8. doi: https://doi.org/10.1148/radiology.197.1.7568850

53. Buckley DL, Drew PJ, Mussurakis S, Monson JR, Horsman A. Microvessel density of invasive breast cancer assessed by dynamic Gd-DTPA enhanced MRI. *J Magn Reson Imaging* 1997; **7**: 461–4. doi: https://doi.org/10.1002/jmri.1880070302
54. Konouchi H, Asaumi JI, Yanagi Y, Shigehara H, Hisatomi M, Matsuzaki H, et al. Evaluation of tumor proliferation using dynamic contrast enhanced-MRI of oral cavity and oropharyngeal squamous cell carcinoma. *Oral Oncol* 2003; **39**: 290–5. doi: https://doi.org/10.1016/S1368-8375(02)00119-7
55. Newbold K, Castellano I, Charles-Edwards E, Mears D, Sohaib A, Leach M, et al. An exploratory study into the role of dynamic contrast-enhanced magnetic resonance imaging or perfusion computed tomography for detection of intratumoral hypoxia in head-and-neck cancer. *Int J Radiat Oncol Biol Phys* 2009; **74**: 29–37. doi: https://doi.org/10.1016/j.ijrobp.2008.07.039
56. Egeland TA, Gaustad JV, Vestvik IK, Benjaminsen IC, Mathiesen B, Rofstad EK. Assessment of fraction of radiobiologically hypoxic cells in human melanoma xenografts by dynamic contrast-enhanced MRI. *Magn Reson Med* 2006; **55**: 874–82. doi: https://doi.org/10.1002/mrm.20852
57. Hoskin PJ, Saunders MI, Goodchild K, Powell ME, Taylor NJ, Baddeley H. Dynamic contrast enhanced magnetic resonance scanning as a predictor of response to accelerated radiotherapy for advanced head and neck cancer. *Br J Radiol* 1999; **72**: 1093–8. doi: https://doi.org/10.1259/bjr.72.863.10700827
58. Bernstein JM, Homer JJ, West CM. Dynamic contrast-enhanced magnetic resonance imaging biomarkers in head and neck cancer: potential to guide treatment? A systematic review. *Oral Oncol* 2014; **50**: 963–70. doi: https://doi.org/10.1016/j.oraloncology.2014.07.011
59. Noij DP, de Jong MC, Mulders LG, Marcus JT, de Bree R, Lavini C, et al. Contrast-enhanced perfusion magnetic resonance imaging for head and neck squamous cell carcinoma: a systematic review. *Oral Oncol* 2015; **51**: 124–38. doi: https://doi.org/10.1016/j.oraloncology.2014.10.016
60. Chawla S, Kim S, Loevner LA, Hwang WT, Weinstein G, Chalian A, et al. Prediction of disease-free survival in patients with squamous cell carcinomas of the head and neck using dynamic contrast-enhanced MR imaging. *AJNR Am J Neuroradiol* 2011; **32**: 778–84. doi: https://doi.org/10.3174/ajnr.A2376
61. Kim S, Loevner LA, Quon H, Kilger A, Sherman E, Weinstein G, et al. Prediction of response to chemoradiation therapy in squamous cell carcinomas of the head and neck using dynamic contrast-enhanced MR imaging. *AJNR Am J Neuroradiol* 2010; **31**: 262–8. doi: https://doi.org/10.3174/ajnr.A1817
62. Shukla-Dave A, Lee NY, Jansen JF, Thaler HT, Stambuk HE, Fury MG, et al. Dynamic contrast-enhanced magnetic resonance imaging as a predictor of outcome in head-and-neck squamous cell carcinoma patients with nodal metastases. *Int J Radiat Oncol Biol Phys* 2012; **82**: 1837–44.
63. Han M, Kim SY, Lee SJ, Choi JW. The correlations between MRI perfusion, diffusion parameters, and 18F-FDG PET metabolic parameters in primary head-and-neck cancer: a cross-sectional analysis in single institute. *Medicine (Baltimore)* 2015; **94**: e2141. doi: https://doi.org/10.1097/md.0000000000002141
64. King AD, Chow SK, Yu KH, Mo FK, Yeung DK, Yuan J, et al. DCE-MRI for pre-treatment prediction and post-treatment assessment of treatment response in sites of squamous cell carcinoma in the head and neck. *PLoS One* 2015; **10**: e0144770. doi: https://doi.org/10.1371/journal.pone.0144770
65. Parker GJ, Roberts C, Macdonald A, Buonaccorsi GA, Cheung S, Buckley DL, et al. Experimentally-derived functional form for a population-averaged high-temporal-resolution arterial input function for dynamic contrast-enhanced MRI. *Magn Reson Med* 2006; **56**: 993–1000. doi: https://doi.org/10.1002/mrm.21066
66. Yu Y, Jiang Q, Miao Y, Li J, Bao S, Wang H, et al. Quantitative analysis of clinical dynamic contrast-enhanced MR imaging for evaluating treatment response in human breast cancer. *Radiology* 2010; **257**: 47–55. doi: https://doi.org/10.1148/radiol.10092169
67. McGrath DM, Bradley DP, Tessier JL, Lacey T, Taylor CJ, Parker GJ. Comparison of model-based arterial input functions for dynamic contrast-enhanced MRI in tumor bearing rats. *Magn Reson Med* 2009; **61**: 1173–84. doi: https://doi.org/10.1002/mrm.21959
68. Mehrabian H, Chandrana C, Pang I, Chopra R, Martel AL. Arterial input function calculation in dynamic contrast-enhanced MRI: an *in vivo* validation study using co-registered contrast-enhanced ultrasound imaging. *Eur Radiol* 2012; **22**: 1735–47. doi: https://doi.org/10.1007/s00330-012-2418-1
69. Cao Y, Popovtzer A, Li D, Chepeha DB, Moyer JS, Prince ME, et al. Early prediction of outcome in advanced head-and-neck cancer based on tumor blood volume alterations during therapy: a prospective study. *Int J Radiat Oncol Biol Phys* 2008; **72**: 1287–90. doi: https://doi.org/10.1016/j.ijrobp.2008.08.024
70. Wang P, Popovtzer A, Eisbruch A, Cao Y. An approach to identify, from DCE MRI, significant subvolumes of tumors related to outcomes in advanced head-and-neck cancer. *Med Phys* 2012; **39**: 5277–9. doi: https://doi.org/10.1118/1.4737022
71. Baer AH, Hoff BA, Srinivasan A, Galban CJ, Mukherji SK. Feasibility analysis of the parametric response map as an early predictor of treatment efficacy in head and neck cancer. *AJNR Am J Neuroradiol* 2015; **36**: 757–62. doi: https://doi.org/10.3174/ajnr.A4296
72. Overgaard J. Hypoxic modification of radiotherapy in squamous cell carcinoma of the head and neck—a systematic review and meta-analysis. *Radiother Oncol* 2011; **100**: 22–32. doi: https://doi.org/10.1016/j.radonc.2011.03.004
73. Wahl RL, Herman JM, Ford E. The promise and pitfalls of positron emission tomography and single-photon emission computed tomography molecular imaging-guided radiation therapy. *Semin Radiat Oncol* 2011; **21**: 88–100. doi: https://doi.org/10.1016/j.semradonc.2010.11.004
74. Rijpkema M, Kaanders J, Joosten F, van der Kogel AJ, Heerschap A. Effects of breathing a hyperoxic hypercapnic gas mixture on blood oxygenation and vascularity of head-and-neck tumors as measured by magnetic resonance imaging. *Int J Radiat Oncol Biol Phys* 2002; **53**: 1185–91. doi: https://doi.org/10.1016/S0360-3016(02)02825-0
75. Kotas M, Schmitt P, Jakob PM, Flentje M. Monitoring of tumor oxygenation changes in head-and-neck carcinoma patients breathing a hyperoxic hypercapnic gas mixture with a noninvasive MRI technique. *Strahlenther Onkol* 2009; **185**: 19–26. doi: https://doi.org/10.1007/s00066-009-1870-6
76. Li XS, Fan HX, Fang H, Song YL, Zhou CW. Value of R2* obtained from T2*-weighted imaging in predicting the prognosis of advanced cervical squamous carcinoma treated with concurrent chemoradiotherapy. *J Magn Reson Imaging* 2015; **42**: 681–8. doi: https://doi.org/10.1002/jmri.24837
77. Panek R, Welsh L, Dunlop A, Wong KH, Riddell AM, Koh DM, et al. Repeatability and sensitivity of T2* measurements in patients with head and neck squamous cell carcinoma at 3T. *J Magn Reson Imaging* 2016; **44**: 72–80. doi: https://doi.org/10.1002/jmri.25134

78. Taylor NJ, Baddeley H, Goodchild KA, Powell ME, Thoumine M, Culver LA, et al. BOLD MRI of human tumor oxygenation during carbogen breathing. *J Magn Reson Imaging* 2001; **14**: 156–63. doi: https://doi.org/10.1002/jmri.1166
79. Rodrigues LM, Howe FA, Griffiths JR, Robinson SP. Tumor R2* is a prognostic indicator of acute radiotherapeutic response in rodent tumors. *J Magn Reson Imaging* 2004; **19**: 482–8. doi: https://doi.org/10.1002/jmri.20024
80. Min M, Lee MT, Lin P, Holloway L, Wijesekera D, Gooneratne D, et al. Assessment of serial multi-parametric functional MRI (diffusion-weighted imaging and R2*) with 18F-FDG-PET in patients with head and neck cancer treated with radiation therapy. *Br J Radiol* 2016; **89**: 20150530. doi: https://doi.org/10.1259/bjr.20150530
81. Koh DM, Blackledge M, Collins DJ, Padhani AR, Wallace T, Wilton B, et al. Reproducibility and changes in the apparent diffusion coefficients of solid tumours treated with combretastatin A4 phosphate and bevacizumab in a two-centre Phase I clinical trial. *Eur Radiol* 2009; **19**: 2728–38. doi: https://doi.org/10.1007/s00330-009-1469-4
82. Messiou C, Orton M, Ang JE, Collins DJ, Morgan VA, Mears D, et al. Advanced solid tumors treated with cediranib: comparison of dynamic contrast-enhanced MR imaging and CT as markers of vascular activity. *Radiology* 2012; **265**: 426–36. doi: https://doi.org/10.1148/radiol.12112565